Journal of Metals, Materials and Minerals, 34(4), 2170, 2024

Single electrode mode triboelectric nanogenerator for recognition of animal sounds

Archana PANDA[1], Kunal Kumar DAS[1], Kushal Ruthvik KAJA[2,*], Mohamed BELAL[3], and Basanta Kumar PANIGRAHI[4,*]

[1] *Department of Electronics and Communication Engineering, Siksha O Anusandhan (deemed to be University), Bhubaneswar 751030, India*
[2] *Department of Physics, Vellore Institute of Technology, Vijayawada 522237, India*
[3] *Graphene Center of Excellence, Energy and Electronics Applications, Egypt-Japan University of Science and Technology, New Borg El-Arab 21934, Egypt*
[4] *Department of Electrical Engineering, Siksha O Anusandhan (deemed to be University), Bhubaneswar 751030, India*

***Corresponding author e-mail**: ruthvik_015@dgist.ac.kr, basantapanigrahi@soa.ac.in

Received date:
3 October 2024
Revised date:
12 October 2024
Accepted date:
21 October 2024

Keywords:
Triboelectric;
Polymer;
Porous;
Animal sound;
Energy harvesting

Abstract

This research presents an innovative and sustainable solution by designing triboelectric nanogenerators (TENGs) for energy harvesting. The fabrication process of TENGs includes PDMS and aluminum. The two single electrode mode TENG was designed one is plain PDMS/Al and the other is porous PDMS/Al TENG devices. The porous PDMS/Al TENG device generated a voltage and current of 7 V and 5 nA for 2 cm × 2 cm device area. Moreover, the TENG system was employed to successfully charge capacitors, and recognize various animal sounds. This study underscores the promising potential of harvesting energy from body movements and powering of devices, paving the way for eco-friendly solutions to energy generation.

1. Introduction

TENG is a device that converts mechanical energy into electrical energy through the triboelectric effect, which occurs when two materials come into contact and then separate, generating an electric charge [1,2]. This innovative technology harnesses everyday mechanical movements, such as walking, vibration, or even wind, and transforms them into usable electrical energy. TENGs are built from simple, cost-effective materials, making them a promising alternative to traditional energy sources for sustainable power generation [3-6]. The principle behind TENGs is based on the combination of triboelectrification and electrostatic induction [7,8]. When two dissimilar materials are rubbed or pressed together, they exchange electrons, creating an imbalance of charge. Once separated, this charge difference can be captured and used as electrical energy. TENGs are highly versatile and can be designed in various forms to suit different applications, including wearable electronics, environmental sensors, and small-scale energy storage systems [9-12]. One key advantage of TENGs is their ability to operate efficiently at low frequencies and in a wide range of environments [13]. By capturing ambient mechanical energy, they offer a sustainable solution for powering portable electronics and contributing to the broader goal of green energy innovation.

TENGs operate in four primary working modes: contact-separation, lateral sliding, single-electrode, and freestanding triboelectric-layer mode [14,15]. Each mode utilizes the triboelectric effect and electrostatic induction to convert mechanical energy into electrical energy, but they differ in how the materials interact and generate charge [16,17]. Among these, the single-electrode mode is often considered the easiest and most practical. It offers a unique blend of simplicity and efficiency in harvesting energy. Their streamlined design allows for easier integration into various devices, making them ideal for wearable technology and compact sensors. Additionally, the grounded electrode can interact with the environment, allowing for more versatile applications. This mode is highly suitable for harvesting energy from irregular human movements, such as walking or hand gestures, making it ideal for wearable and portable energy solutions. Recently Behera *et al.* used EVA: BFO composite for the TENG fabrication and performed under single electrode mode. The device achieved an output of 45 V and 800 nA [18]. In another study, Vivekananthan *et al.* developed a TENG by PVDF and achieved an output of 50 V and 600 nA respectively [19]. Padhan *et al.* fabricated a single electrode TENG using a ferromagnetic composite and achieved a voltage of 62 V and a current of 250 nA. The prepared device is successfully able to turn on the LEDs and small electronics [20].

TENGs harvest energy from human body movements offering clean and renewable energy sources by generating power from routine actions like jogging, walking, or even basic hand movements [21-23]. This energy can be stored and reuse for powering of consumer electronics without the need for conventional batteries or external charging [24-26]. Wildlife monitoring can likewise benefit greatly

from TENG-based equipment. These sensors can follow an animal's movements and behaviors or even notify humans of changes in the surrounding environment by listening to sound signals from the animal. Accurate sound detection helps researchers understand how animals communicate and warns against poaching and ecological disturbance. TENG-based acoustic sensors can operate in remote locations and provide continuous, real-time data [27-30].

In this work, a soft lithographic technique was utilized for fabrication of porous TENG. Two device performance based on plain PDMS and porous PDMS alongside Al was being compared. The single electrode mode operating mode was chosen for easy operation. The electrical performance was compared for both prepared devices and further this device was utilized to harvest energy from body movements. Animal noise detection was carried out to showcase the utilization of TENG in real time operations.

2. Synthesis and experimental techniques

The PDMS was prepared using mixing of Monomer: hardener ratio 10:1. The chemical was procured from DOW, USA (slygard 184). After mixing and obtaining a transparent solution it was casted over a perti plate. Further, it was placed inside an oven at 60°C for 3 h to obtained a free standing plain film. For the porous PDMS instead of Petri plate the solution was casted upon a 200 grit sandpaper which lead to transfer of micro roughness on one side of PDMS which acted as negative triboelectric layer. The positive triboelectric layer was considered as double sided conductive aluminum tape. The device active area was taken as 2 cm × 2 cm. Using an X-ray diffractometer (Rigaku Miniflex, Japan), X-ray diffraction (XRD) patterns were obtained at room temperature for PDMS in order to study the phase formation. The micrographs of porous and plain PDMS were examined using a (FESEM, ZEISS) to obtain energy dispersive X-ray (EDX) spectra and scanning electron microscopy (SEM) pictures. Using data from a phase-sensitive meter (PSM 1735 N4L), the dielectric constant was evaluted. This examination shed light on the electrical properties of the materials under investigation. The TENG electrical signals were captured using Keithley Electrometer 6514 and homemade LabVIEW program. The period force applied to device was done using a linear motor (LINMOT, USA). The speakers were purchased from Zebronics, India.

3. Results and discussion

Figure 1(a-b) shows the microstructure and elemental mapping of the plain PDMS film. The microstructure of plain PDMS is characterized by a smooth, flexible, and elastomeric surface with a homogeneous distribution of polymer chains. It exhibits low surface roughness and lacks significant porosity or crystalline features. This structure makes PDMS highly suitable for applications requiring flexibility, transparency, and biocompatibility [31]. The elements such as Si, O, C are present uniformly over the surface of PDMS without any impurity. Figure 1(c-d) shows the microstructure and elemental mapping of the porous PDMS film. Introducing a porous microstructure in PDMS using sandpaper can significantly enhance the performance of TENGs. The roughened, porous surface increases the surface area, leading to more contact points during triboelectric interactions. This results in a higher charge density and improves the efficiency of charge transfer between materials.

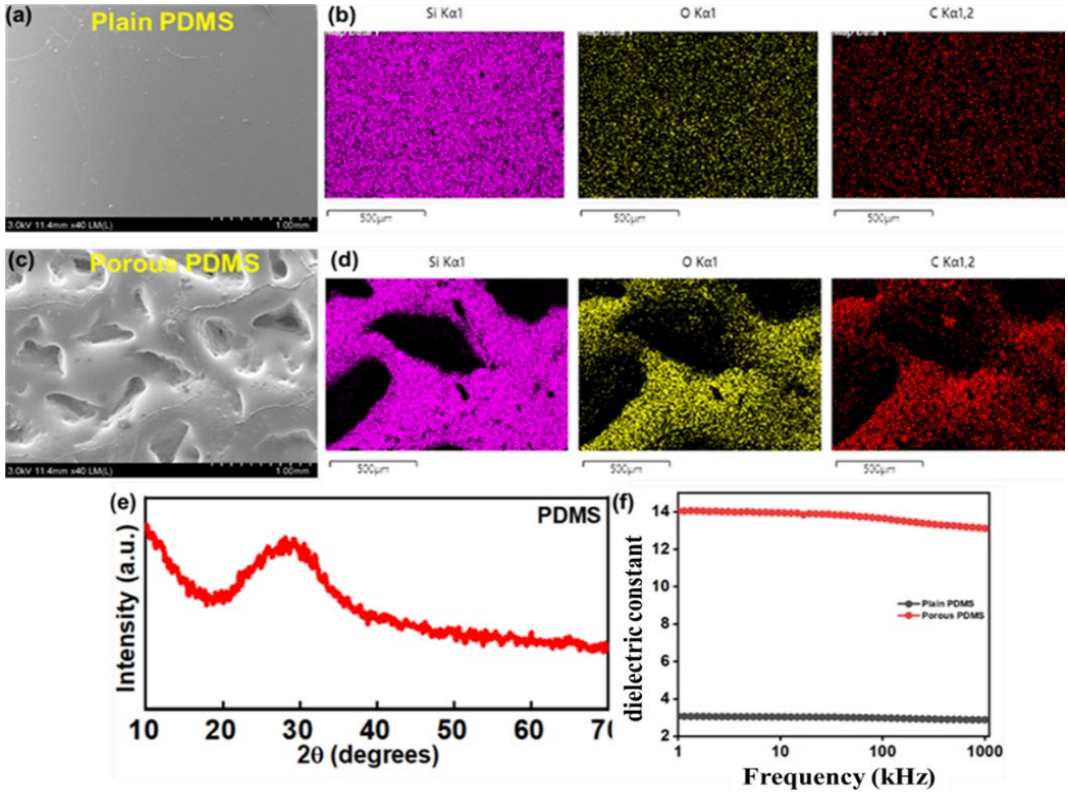

Figure 1. (a, b) Micrographs of plain PDMS and corresponding elemental mapping of elements, (c, d) Micrographs of porous PDMS and corresponding elemental mapping of elements, (e) XRD spectra of PDMS, and (f) dielectric constant of the plain PDMS and porous PDMS.

Figure 1(e) shows the XRD pattern of PDMS film. XRD analysis of PDMS typically shows broad, low-intensity peaks due to its amorphous nature. In PDMS, a broader peak appears around 2θ~21° [32]. This peak indicates short-range structural order, which is characteristic of amorphous silica. It corresponds to the spacing between silicon atoms within the PDMS backbone, highlighting the material's partial structural organization despite its overall amorphous nature. The scan rate used for XRD is $2°\cdot min^{-1}$ and the voltage used in SEM is 3 kV. Figure 1(f) shows the dielectric constant of pure PDMS and porous PDMS samples. The electric constant of plain PDMS was about 3.1 at 1 kHz whereas for porous PDMS it improved by 14 at 1 kHz. The dielectric constant of porous PDMS is higher than that of plain PDMS because of its larger surface area and air-filled pores. By increasing polarization in the presence of an electric field, these pores increase charge storage capacity. In comparison to the solid, non-porous PDMS, the voids within the porous structure contribute to higher dielectric permittivity.

Figure 2(a-d) shows the single electrode mode operation of TENG. Triboelectrification and electrostatic induction are the foundations of a TENG operation. The moving layer in the single-electrode TENG mechanism depicted in Figure 2 is aluminum. When both triboelectric layers are connected each opposite layer develop the charges on the surface as per the polarity (a). A sizable potential difference between the two layers develops as the Al layer separates from the PDMS surface, which causes electrons to travel from the ground to the Al electrode (b). Until the Al and PDMS layers revert to their initial places, this electron flow will continue (c). The direction of electron flow changes as the Al layer approaches the PDMS layer again, moving. The pores in the PDMS layer play a key role in increasing surface charge density, thereby enhancing the TENG's output.

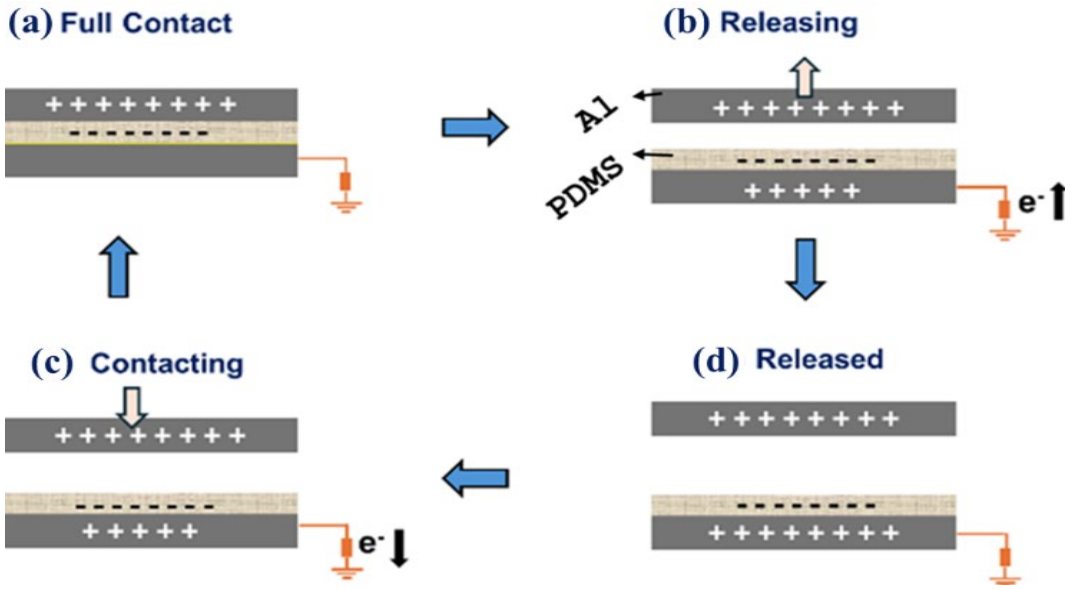

Figure 2. Working mechanism of the single electrode TENG.

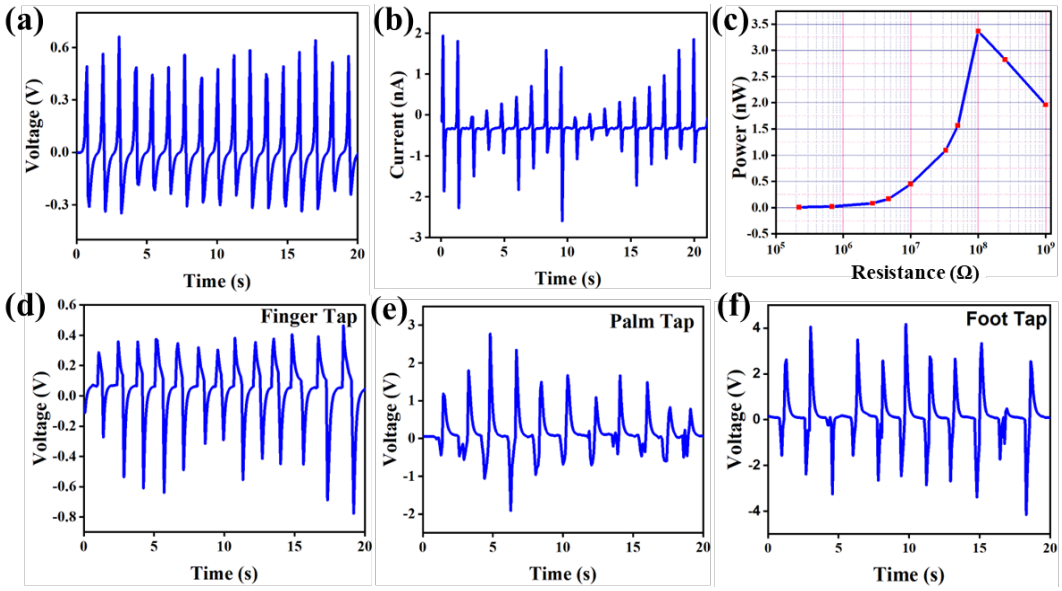

Figure 3. (a, b) Voltage and current of the plain PDMS/Al TENG device, (c) Power generated by the TENG, and (d-f) Voltage output of the plain PDMS/Al TENG device.

The fabricated TENGs were operated in single-electrode mode. The plain PDMS-based TENG achieved an output of 1 V and 4.5 nA, as shown in Figure 3(a-b). The power was calculated using the formula V^2/R and was found to be 3.3 nW, corresponding to 10 MΩ, as shown in Figure 3(c). The TENG was then attached to the human body to harness energy from human motion. Figure 3(d-f) show the voltage generated by the TENG in response to different actions such as finger tapping, palm tapping, and foot tapping. As the roughness of the film increased, the output of the TENG improved. The porous PDMS-based TENG achieved an output voltage of 7 V and a current of 5 nA, as shown in Figure 4(a-b). The calculated power for the porous PDMS-based TENG was 165 nW, corresponding to 5 MΩ, as illustrated in Figure 4(c). Figure 4(d-f) demonstrate the voltage generated by the TENG during various human actions.

Figure 5(a) shows the circuit diagram of capacitor charging using TENG and bridge rectifier. The bridge rectifier enable the conversion of AC output of TENG to DC. Figure 5(b-c) illustrated the various capacitors being charged using plain PDMS and porous PDMS respectively. Porous PDMS-based TENGs charge capacitors more quickly due to their enhanced surface area and increased contact points, which lead to higher charge generation and transfer efficiency. The porous structure improves friction and contact with the other triboelectric layer, resulting in greater charge density. This, in turn, accelerates the charging process of capacitors by delivering higher energy output with each cycle. Figure 5(d) shows the digital image of the TENG being attached to the speakers for animal noise detection. Animal noise detection is crucial for monitoring wildlife behavior, tracking species in their natural habitats, and understanding communication patterns [33].

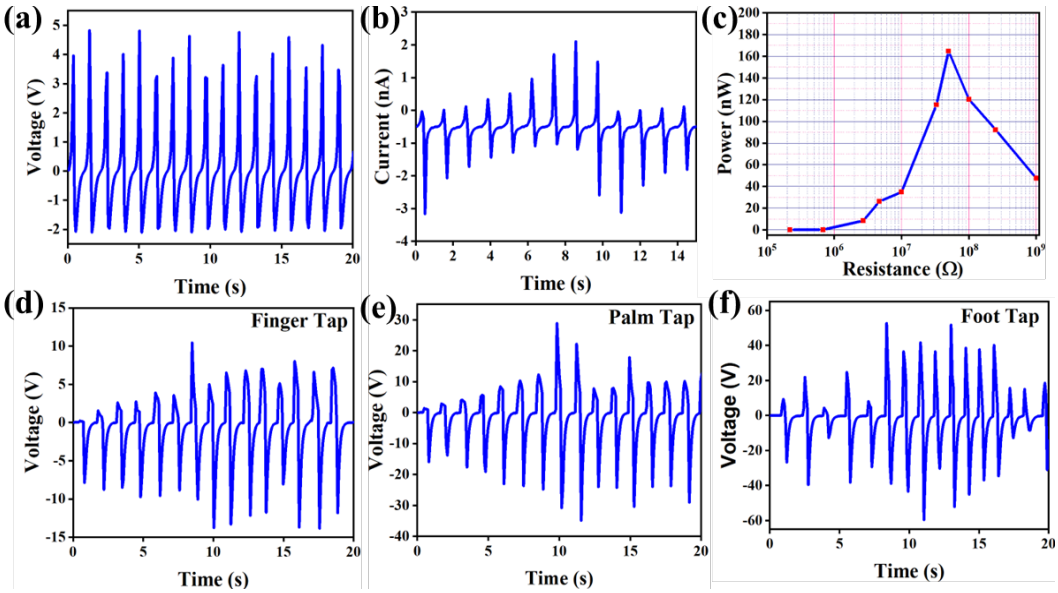

Figure 4. (a, b) Voltage and current of the porous PDMS/Al TENG device, (c) Power generated by the TENG, and (d-f) Voltage output of the porous PDMS/Al TENG device.

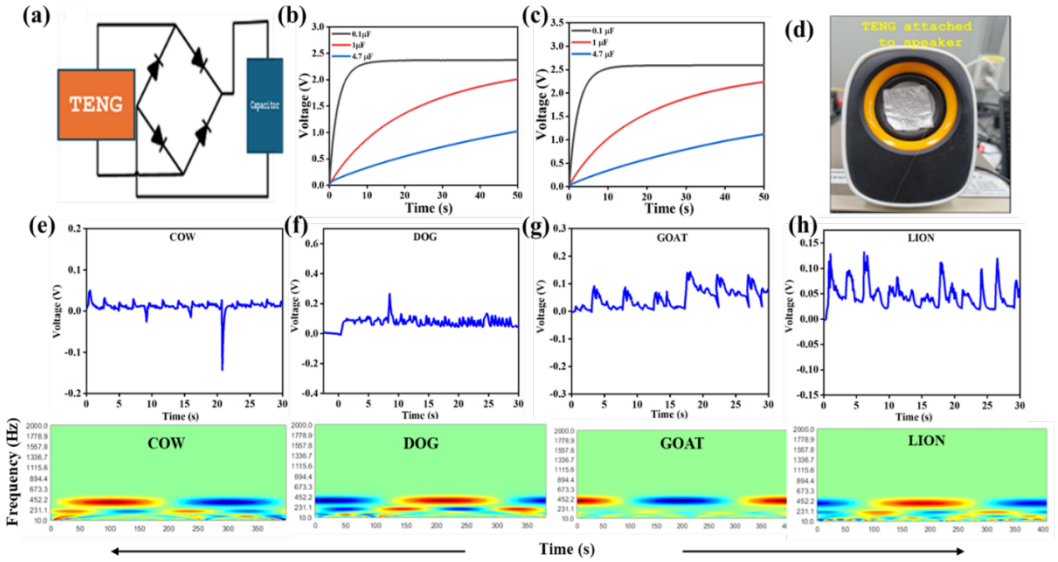

Figure 5. (a) Circuit design of connection of TENG and charge of capacitor, (b, c) charging of commercial capacitors using plain PDMS/Al device and porous PDMS/Al device, (d) digital image of porous PDMS/Al TENG device attached to the speaker for noise detection, (e-h) Voltage signal and computational analysis from TENG during various roaring of animals such as cow, dog, goat, lion.

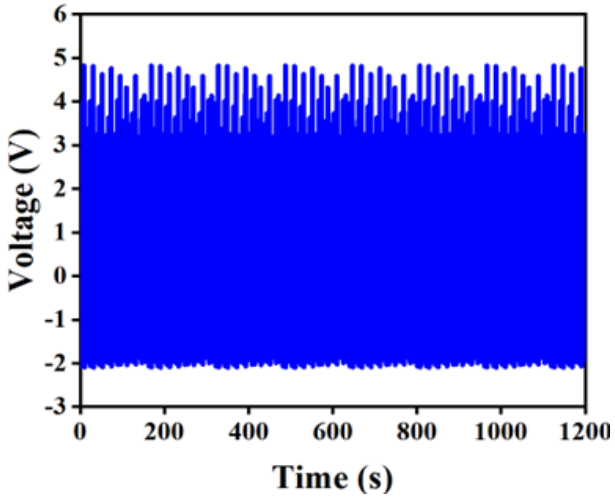

Figure 6. Stability test over 1000 cycles.

It aids in conservation efforts by identifying endangered species, detecting environmental changes, and preventing illegal activities like poaching. Additionally, it contributes to research in bioacoustics and ecological studies. Figure 5(e-h) shows the voltage and computational analysis of TENG during the noise detection of various animal such as cow, dog, goat and lion. Changes in signal can be seen from output of TENG which can help in real time biodiversity monitoring. The stability of porous PDMS-based TENG was tested over 1000 cycles, demonstrating excellent performance and durability is shown in Figure 6.

4. Conclusions

This study explores the use of TENG technology for sustainable, battery-free noise detection sensors, ideal for applications like animal behavior monitoring or biodiversity monitoring. PDMS materials, processed via the solvent casting route. PDMS roughness was introduced by using sandpaper microroughness treatment. TENG devices with plain PDMS, porous PDMS and Al layers were created to compare electrical output. The device demonstrated potential for charging capacitors, while also successfully performing self-powered noise recognition sensing and energy harvesting utilizing human activities..

References

[1] A. Kulandaivel, S. Potu, A. Babu, M. Navaneeth, V. Mahesh, R. R. Kumar, and U. K. Khanapuram, "Advances in ferrofluid-based triboelectric nanogenerators: Design, performance, and prospects for energy harvesting applications," *Nano Energy*, vol. 120, p. 109110, 2024.

[2] T. Charoonsuk, S. Pongampai, P. Pakawanit, and N. Vittayakorn, "Achieving a highly efficient chitosan-based triboelectric nanogenerator via adding organic proteins: Influence of morphology and molecular structure," *Nano Energy*, vol. 89, p. 106430, 2021.

[3] M. Sahu, S. Hajra, H.-G. Kim, H.-G. Rubahn, Y. Kumar Mishra, and H. J. Kim, "Additive manufacturing-based recycling of laboratory waste into energy harvesting device for self-powered applications," *Nano Energy*, vol. 88, p. 106255, 2021.

[4] S. Panda, S. Hajra, Y. Oh, W. Oh, J. Lee, H. Shin, V. Vivekananthan, Y. Yang, Y. K. Mishra, and H. J. Kim, "Hybrid nanogenerators for ocean energy harvesting: Mechanisms, designs, and applications," *Small*, vol. 19, no. 25, p. 2300847, 2023.

[5] E. Elsanadidy, I. M. Mosa, D. Luo, X. Xiao, J. Chen, Z. L. Wang, and J. F. Rusling, "Advances in triboelectric nanogenerators for self-powered neuromodulation," *Advanced Functional Materials,* p. 2211177, 2023.

[6] Y. Wei, X. Li, Z. Yang, J. Shao, Z. L. Wang, and D. Wei, "Contact electrification at the solid–liquid transition interface," *Materials Today*, 2024.

[7] Z. L. Wang, and A. C. Wang, "On the origin of contact-electrification," *Materials Today*, vol. 30, pp. 34-51, 2019.

[8] H. Zou, Y. Zhang, L. Guo, P. Wang, X. He, G. Dai, H. Zheng, C. Chen, A. C. Wang, C. Xu, and Z. L. Wang, "Quantifying the triboelectric series," *Nature Communications*, vol. 10, no. 1, p. 1427, 2019.

[9] R. Khwanming, S. Pongampai, N. Vittayakorn, and T. Charoonsuk, "Cellulose-based fabrics triboelectric nanogenerator: Effect of fabric microstructure on its electrical output," *Journal of Metals, Materials and Minerals*, vol. 33, no. 3, p. 1673, 2023.

[10] G. Yadav, K. Jindal, and M. Tomar, "Fabrication of GaN-based MSM droplet triboelectric nanogenerator by the conjunction of photovoltaic and triboelectric effect," *Journal of Alloys and Compounds*, vol. 944, p. 169178, 2023.

[11] K. Ruthvik, A. Babu, S. Potu, M. Navaneeth, V. Mahesh, U. K. Khanapuram, R. R. Kumar, B. M. Rao, H. Divi, and K. Prakash, "High-performance triboelectric nanogenerator based on 2D graphitic carbon nitride for self-powered electronic devices," *Materials Letters*, vol. 350, p. 134947, 2023.

[12] A. Babu, K. Ruthvik, P. Supraja, M. Navaneeth, K. U. Kumar, R. R. Kumar, K. Prakash, and N. Raju, "High-performance triboelectric nanogenerator using ZIF-67/PVDF hybrid film for energy harvesting," *Journal of Materials Science: Materials in Electronics*, vol. 34, no. 33, p. 2195, 2023.

[13] K. N. Kim, S. Y. Kim, S. H. Choi, M. Lee, W. Song, J. Lim, S. S. Lee, and S. Myung, "All-printed wearable triboelectric nanogenerator with ultra-charged electron accumulation polymers based on MXene nanoflakes," *Advanced Electronic Materials*, vol. 8, no. 12, p. 2200819, 2022.

[14] W. Liu, Z. Wang, and C. Hu, "Advanced designs for output improvement of triboelectric nanogenerator system," *Materials Today*, vol. 45, pp. 93-119, 2021.

[15] J. A. L. Jayarathna, and K. R. Kaja, "Energy-Harvesting device based on lead-free perovskite," *AI, Computer Science and Robotics Technology,* vol. 3, 2024.

[16] W.-G. Kim, D.-W. Kim, I.-W. Tcho, J.-K. Kim, M.-S. Kim, and Y.-K. Choi, "Triboelectric nanogenerator: Structure, mechanism, and applications," *ACS Nano*, vol. 15, no. 1, pp. 258-287, 2021.

[17] N. Kumar, B. Mahale, T. S. Muzata, and R. Ranjan, "Energy harvesting with flexible piezocomposite fabricated from a biodegradable polymer," *International Journal of Energy Research*, vol. 45, no. 13, pp. 19395-19404, 2021.

[18] S. A. Behera, S. Hajra, S. Panda, A. K. Sahu, P. Alagarsamy, Y. K. Mishra, H. J. Kim, and P. G. R. Achary, "Synergistic

energy harvesting and humidity sensing with single electrode triboelectric nanogenerator," *Ceramics International*, vol. 50, no. 19, pp. 37193-37200, 2024.

[19] V. Vivekananthan, S. Arunmetha, S. Srither, P. S. S. Babu, S. Hajra, and B. Dudem, "A highly wearable single-electrode mode triboelectric nanogenerator made of flexible polyvinylidene fluoride transparent film for muscular motion monitoring," *Journal of Physics: Conference Series*, vol. 2471, no. 1: IOP Publishing, p. 012025, 2023.

[20] A. M. Padhan, S. Hajra, M. Sahu, S. Nayak, H. J. Kim, and P. Alagarsamy, "Single-electrode mode TENG using ferromagnetic NiO-Ti based nanocomposite for effective energy harvesting," *Materials Letters*, vol. 312, p. 131644, 2022.

[21] Y. Yun, S. Jang, S. Cho, S. H. Lee, H. J. Hwang, and D. Choi, "Exo-shoe triboelectric nanogenerator: Toward high-performance wearable biomechanical energy harvester," *Nano Energy*, vol. 80, p. 105525, 2021.

[22] S. Hajra, S. Panda, H. Khanberh, V. Vivekananthan, E. Chamanehpour, Y. K. Mishra, and H. J. Kim, "Revolutionizing self-powered robotic systems with triboelectric nanogenerators," *Nano Energy*, vol. 115, p. 108729, 2023.

[23] M. Rakshita, M. Navaneeth, A. S. Aachal, P. P. Payal, A. K. Durga Prasad Kasireddi, K. K. Uday, R. K. Rajaboina, and D. Haranath, "Phosphor-based triboelectric nanogenerators for mechanical energy harvesting and self-powered systems," *ACS Applied Electronic Materials*, vol. 6, no. 3, pp. 1821-1828, 2024.

[24] G. Cai, X. Wang, M. Cui, P. Darmawan, J. Wang, A. Lee-Sie Eh, and P. S. Lee, " Electrochromo-supercapacitor based on direct growth of NiO nanoparticles," *Nano Energy*, vol. 12, pp. 258-267, 2015.

[25] M. Waseem, M. Ahmad, A. Parveen, and M. Suhaib, "Battery technologies and functionality of battery management system for EVs: Current status, key challenges, and future prospectives," *Journal of Power Sources*, vol. 580, p. 233349, 2023.

[26] K. Lolupima, J. Cao, D. Zhang, C. Yang, X. Zhang, and J. Qin, "A review on the development of metals-doped Vanadium oxides for zinc-ion battery," *Journal of Metals, Materials and Minerals*, vol. 34, no. 3, p. 2084, 2024.

[27] M. Yuan, C. Li, H. Liu, Q. Xu, and Y. Xie, "A 3D-printed acoustic triboelectric nanogenerator for quarter-wavelength acoustic energy harvesting and self-powered edge sensing," *Nano Energy*, vol. 85, p. 105962, 2021.

[28] H.-S. Kim, N. Kumar, J.-J. Choi, W.-H. Yoon, S. N. Yi, and J. Jang, "Self-powered smart proximity-detection system based on a hybrid magneto-mechano-electric generator," *Advanced Intelligent Systems*, vol. 6, no. 1, p. 2300474, 2024.

[29] M. Cui, H. Guo, W. Zhai, C. Liu, C. Shen, and K. Dai, "Template-assisted electrospun ordered hierarchical microhump arrays-based multifunctional triboelectric nanogenerator for tactile sensing and animal voice-emotion identification," *Advanced Functional Materials*, vol. 33, no. 46, p. 2301589, 2023.

[30] A. Babu, S. Gupta, R. Katru, N. Madathil, A. Kulandaivel, P. Kodali, H. Divi, H. Borkar, U. K. Khanapuram, and R. K. Rajaboina "From acoustic to electric: Advanced triboelectric nanogenerators with fe-based metal–organic frameworks," *Energy Technology*, vol. 12, no. 8, p. 2400796, 2024.

[31] I. Miranda, A. Souza, P. Sousa, J. Ribeiro, E. M. Castanheira, R. Lima, and G. Minas, "Properties and applications of PDMS for biomedical engineering: A review," (in eng), *Journal of Functional Biomaterials*, vol. 13, no. 1, 2021.

[32] P. Ferreira, Á. Carvalho, T. R. Correia, B. P. Antunes, I. J. Correia, and P. Alves, "Functionalization of polydimethylsiloxane membranes to be used in the production of voice prostheses," *Science and Technology of Advanced Materials*, vol. 14, no. 5, p. 055006, 2013.

[33] I. Nolasco, S. Singh, V. Morfi, V. Lostanlen, A. Strandburg-Peshkin, E. Vidaña-Vila, L. Gill, H. Pamuła, H. Whitehead, I. Kiskin, F. H. Jensen, J. Morford, M. G. Emmerson, E. Versace, E. Grout, H. Liu, B. Ghani, D. Stowell, "Learning to detect an animal sound from five examples," *Ecological Informatics*, vol. 77, p. 102258, 2023.